ELSEVIER

Clinical Neurophysiology 110 (1999) 1410–1426

Instantaneous EEG coherence analysis during the Stroop task

B. Schack[a,*], A.C.N. Chen[b], S. Mescha[a], H. Witte[a]

[a]*Institute of Medical Statistics, Computer Science and Documentation, University of Jena, Jahnstraza 3, D-07740 Jena, Germany*
[b]*Human Brain Mapping and Cortical Imaging Laboratory, Centre for Sensory-Motor Interaction, Aalborg University, Aalborg, DK 9220, Denmark*

Accepted 19 April 1999

Abstract

Objective: In the present study the Stroop effect is analyzed by means of EEG coherence analysis in addition to traditional analysis of behavioral data (reaction time) and ERP analysis. Data from 10 normal subjects are examined.

Methods: In particular, a special dynamic approach for a continuous coherence estimation is applied to investigate the procedural evolution of functional cortical relationships during the Stroop task.

Results: The frequency band of 13–20 Hz is found to be sensitive to the discrimination between the congruent and the incongruent task conditions on the basis of instantaneous coherence analysis. The magnitude of coherence values within the time interval of late potentials and the maximal coherence values are used to assess the strength of interaction between distinct areas of the cortex. Higher coherences are observed within the left frontal and left parietal areas, as well as between them for the incongruent situation in comparison with the congruent situation. Furthermore, the time-points of maximal coherence allows a procedural discrimination between both situations. The peak synchrony described by the time-points of maximal coherence correlates strongly with the reaction times mainly within the frontal area and between fronto-parietal areas in the incongruent case, whereas this correlation is restricted to the right hemisphere in the congruent case.

Keywords: Stroop task; Frontal and parietal area of the cortex; Hemispheres; Event-related potentials; Instantaneous EEG coherence

1. Introduction

In the Stroop color-word task subjects are confronted with words written in different colors and are asked to name the colors as quickly as possible while ignoring the words themselves. In the standard version of the task Stroop (1935) the words are color names and are written in incongruent colors (e.g. the word RED written in blue ink).

The interference of the word with color-naming is a reliable phenomenon. Not only is response time longer but the errors in naming are more numerous. The fact that word-reading is generally faster than color-naming in non-conflict, i.e. congruent situations, suggests an explanation of what is happening, namely that the stronger habit of reading words is difficult to suppress and must be inhibited before the color-naming response can be made.

Depending on the hypothesized locus of the Stroop effect, three classes of explanations can be distinguished.

1. Hock and Egeth (1970) suggest that the color-word disrupts the identification of the color by diverting attention from it. This 'distraction effect' is largest for words semantically related to the color-naming task because the subjects are sensitized to them. The most important objection against this perceptual-encoding hypothesis is that it cannot explain why the congruent stimuli do not cause interference although the semantic similarity between word and color is maximal.
2. The response-competition hypothesis of the Stroop phenomenon (Morton, 1969; Keele, 1972; Warren, 1972; Posner and Snyder, 1975) states that word and color are processed in a parallel manner until their motor programs are activated. As only the program that corresponds to the relevant stimulus dimensions is admitted to response execution, the program that corresponds to the irrelevant stimulus dimension must be prevented from gaining control over the overt response. There is no conflict when congruent stimuli are to be named or read, because both stimulus components activate the same response program. Neither does reading incongruent stimuli provide a problem as the relevant motor program reaches the execution stage before the

* Corresponding author. Tel.: + 49-3641-9-33651; fax: + 49-3641-9-33200.
E-mail address: irc@imsid.uni-jena.de (B. Schack)

1388-2457/99/$ - see front matter
CLINPH 98606
PII: S1388-2457(99)00111-X

irrelevant one does. If, on the other hand, incongruent stimuli have to be named, the irrelevant motor code arrive at the response execution stage before the relevant one does. The delay in reaction time and the other behavioral signs of a conflict are explained as a consequence of the subject's difficulty in suppressing the first and executing the second of two articulatory codes that arrive at the response execution stage in close succession.

3. Contradicting this view, however, are experimental findings that suggest that the main conflict occurs at an earlier stage when the color information makes contact with semantic memory after perceptual encoding. These results support a semantic-encoding hypothesis as proposed bySeymour, 1974,1977). The simultaneous activation of two distinct semantic codes that are closely related leads to an ambiguity that must be resolved before further processing. The Stroop phenomenon is an indication of the extra processing time needed to delete the irrelevant code. Processing congruent stimuli causes no response delay because both components of the stimulus activate the same semantic code.

All three explanations are related to the observation of longer reaction time due to the Stroop effect. This behavioral parameter indicates different information processes with regard to their time evolution in incongruent and congruent cases.

In order to connect the time information simultaneously with the topographic information, the event-related potentials method has been proposed for studying the Stroop effect. The P3 latency and the level of negativity of late potentials in particular were examined in order to investigate the locus of interference in the Stroop task. Differences with regard to the Stroop effect were found mainly for the parietal electrode positions (Warren and Marsch, 1979; Czigler and Csibra 1991; Soininen et al., 1995). Further, EEG power for different frequency bands of the frontal and parietal regions were implicated in these examinations (Hasenfratz and Bättig 1992; Willis et al., 1996; West and Bell, 1997). Hasenfratz and Bättig (1992) found a significant influence of smoking and caffeine on the Stroop effect primarily for increased Beta-power (12–25 Hz) for the electrodes P3 and P4. West and Bell (1997) observed an increased Alpha1-power (8–10 Hz) within the prefrontal and parietal areas and assumed an interaction between prefrontal and parietal regions.

In order to get topological information about the Stroop effect, modern imaging methods such as PET and fMRI have been applied during the Stroop task. The neuroimaging studies indicated that the prefrontal cortex is closely involved in the performance of the Stroop task (see e.g. Bench et al., 1993). In medical approaches functional imaging techniques have been increasingly used for exploring the relationship between brain activity and particular psychological functions (in normal volunteers) or symptoms (in psychiatric patients). Resting-state studies in patients with depression, in whom attentional deficits are common, have identified cingulate abnormalities (Bench et al., 1993; Taylor et al., 1994). Furthermore, abnormalities in Stroop test performance have frequently been used to indicate frontal dysfunctions in patients without clear focal frontal lesions, for instance on the basis of MRI measurements (Vrendell et al., 1995).

The three different approaches – analysis of behavioral data, ERP-analysis and neuroimaging techniques – serve the examination of the Stroop task, either for the time behavior of this information process or for the location within the cortex area. An investigation of the functional relationship between different areas of the cortex is not possible on the basis of these methods.

The aim of this study is the detection of interaction processes of different brain instances during the Stroop task in relation to the time-evolution of the cognitive process on the basis of instantaneous coherence analysis. Interactions are expected within and between the left frontal and parietal topographic areas due to the fact that frontal areas are strongly implicated in the execution of frontal functions, such as planning and response selection, and, further, left parietal area may also be implicated since the Stroop task utilizes color-word perception and retrieval of semantic memory.

First, the Stroop effect will be examined with regard to the reaction time and ERP to show comparability with prior behavioral and EEG studies.

The aims, with respect to the coherence analysis, are as follows:

1. First of all, the existence of a frequency band for the discrimination between the two task-situations by means of the coherence has to be considered with regard to frontal and parietal topographic areas,
2. Further, starting from the results of the ERP analysis with regard to late potentials, the interactions of different topographic areas of the cortex during the second half of the task (400 ms by the end of the task) will be investigated by means of calculating the values of coherence of the sensitive frequency band in order to examine the Stroop effect.
3. The question of a correlation between the reaction time as an external parameter and the time of maximal interaction (described by the time-point of maximal coherence) as an internal parameter of the information process during the Stroop task arises. A high correlation between these two time parameters would indicate interaction processes as characteristic events associated with the Stroop task.
4. Topographic differences between congruent and incongruent task-situations will be analyzed with regard to the strength of the correlation between reaction time and the time-point of maximal coherence and the strength of interaction described by the maximal coherence.

2. Materials and methods

2.1. Subjects

Ten, healthy right-handed male undergraduate and graduate student volunteers (aged 20–30) participated in the study. Each subject was free from neurological or psychiatric disorders, had a normal EEG, and gave his written informed consent to take part in the project in accordance with the Helsinki Declaration. None of the subjects was familiar with the aims of the research work.

2.2. EEG session

The EEG was recorded from the scalp by means of a 19 non-polarizable Ag–AgCl electrode-cap using the Neuro Scan Medical System (10/20-Systems, Impedance <5 KΩ, sampling frequency at 250 Hz, bandpass of 0.1–50 Hz, 16 bit resolution). Simultaneously the electrooculogram (EOG) was recorded on one additional channel. EOG artifacts were selected by correlation analysis between the EOG and the EEG, as well as by visual control. Only trials without artifacts were included in further data-processing.

In order to ensure the comparability with the results of other EEG studies of the Stroop task the unipolar derivation with linked ear-lobes as reference was used (e.g. Warren and Marsch, 1979; Czigler and Csibra, 1991; Hasenfratz and Bättig 1992).

2.3. Task design

The subject sits in front of a 17″ computer screen, where color words are presented written in ink of different colors. The task-order of congruent cases, such as the word 'red' written in red ink, and incongruent cases, such as the word 'red' written in blue ink, was random. The subject has to name the color as quickly as possible. The number of tasks was 21 for the congruent case and 29 for the incongruent case. The answers were recorded with a microphone continuously in time in order to detect erroneous answers and to register the reaction time (RT).

2.4. Methods

In addition to the procedural investigation by means of event-related potentials, an adaptive estimation method of the coherence function is used which allows a high time and frequency resolution. This general method of estimating instantaneous coherence was developed in Schack et al. (1995). The basic idea of the method is as follows: a pair of EEG channels is understood as a two-dimensional instationary signal process. This process is modeled as a two-dimensional autoregressive moving-average model with time-dependent parameters. The optimization criterion for adapting parameters is the minimization of the prediction error of the model in the least mean square sense. The correction of the model according to this criterion is performed at every sample point. Thus, the parameters of the model are functions of time and allow the parametric calculation of the momentary spectral density matrix of the ARMA model, which approximates the spectral density matrix of the underlying pair of EEG channels for the momentary time-point. Subsequently, the continuous estimation of the coherence is derived from the momentary

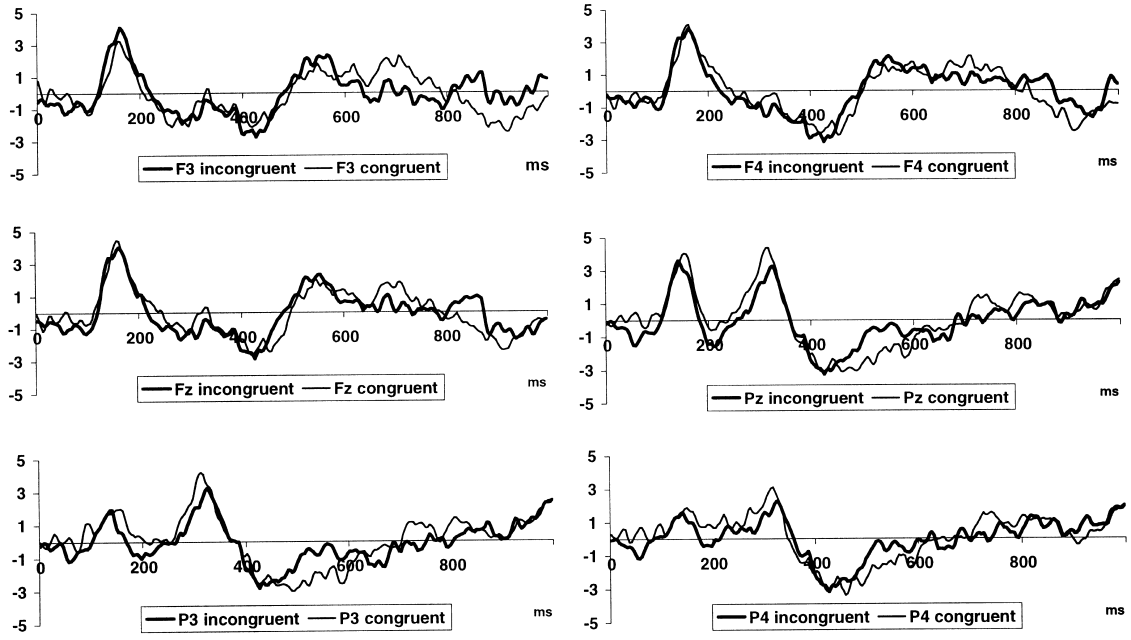

Fig. 1. ERP (in μV) of the Stroop task for incongruent (bold curves) and congruent (thin curves) situations for the frontal electrode positions F3, F4 (upper panels), for the fronto- and parieto-central electrode positions Fz and Pz (middle panels) and for the parietal electrode positions P3 and P4 (panels below).

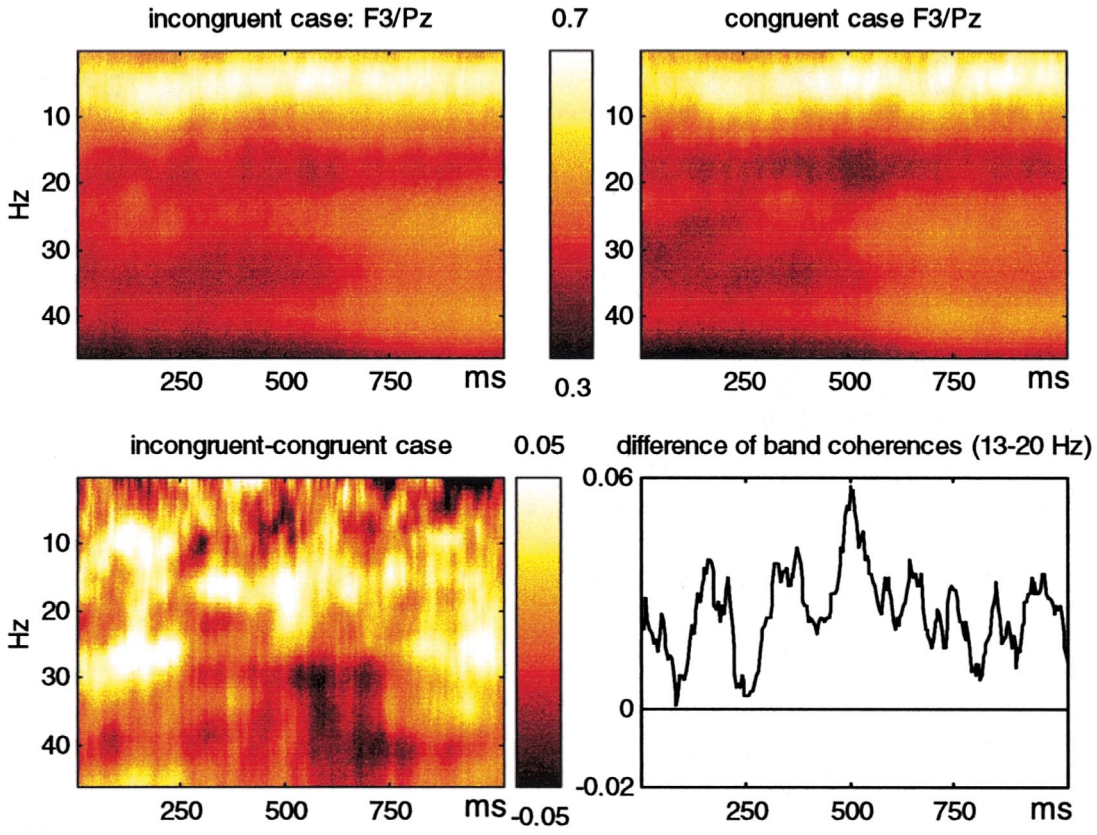

Fig. 2. Time-frequency-analyses of instantaneous coherence of the electrode pair F3/Pz for the incongruent (upper left panel) and congruent (upper right panel) situations. In the lower left panel the difference (incongruent-congruent) between them is illustrated. The lower right panel shows the time course of the difference between the band coherences (incongruent-congruent) for the frequency band 13–20 Hz. The average of the time-frequency-matrices and the band coherences was performed for all single trials and all 10 subjects.

spectral density matrix of the fitted ARMA model. Although the correction will be performed at every sample point, a smearing of the time evolution of the coherence estimation cannot be prevented. The continuous coherence estimation depends on the past with an exponentially decreasing memory. Nevertheless, the time resolution is much higher than that for estimation methods on the basis of the Fourier transformation. The interested reader can find the detailed estimation procedure in Schack (1999); Schack et al. (1999a) and a short description in the Appendix. This approach allows the time-dependent calculation of the full coherence spectrum and therefore the predefinition of a sensitive frequency band for the investigation of the information processing considered.

The coherence analysis was performed for 30 adjacent electrode pairs in the longitudinal and transversal directions – so-called local coherences – and additionally for 9 fronto-parietal electrode pairs F3/P3, F3/Pz, F3/P4, Fz/P3, Fz/Pz, Fz/P4, F4/P3, F4/Pz and F4/P4. For a topographic presentation of local synchronization processes the mapping procedure for local coherences was used (Rappelsberger and Petsche, 1988). With this aim, fictive coherence positions were placed in the middle of the 30 adjacent electrode pairs considered. The linear interpolation procedure led to the local coherence map.

3. Results

3.1. Behavioral data

The well-known Stroop effect for the reaction times could be verified in our examination. The mean reaction times and the correspondent standard deviations of 10 subjects were, for the incongruent task, 793 ms (109 ms SD) and for the congruent task 708 ms (114 ms SD) Thus, the mean duration of the incongruent task was 85 ms longer than the duration of the congruent task. This difference in reaction time is significantly high (paired samples t test at the significance level of 1%).

3.2. Event-related potentials

Fig. 1 shows the event-related potentials for selected electrode positions within the frontal and parietal area. Differences appear for the late potentials 400-600 ms after the presentation of the word in the parietal regions (see Fig. 1).

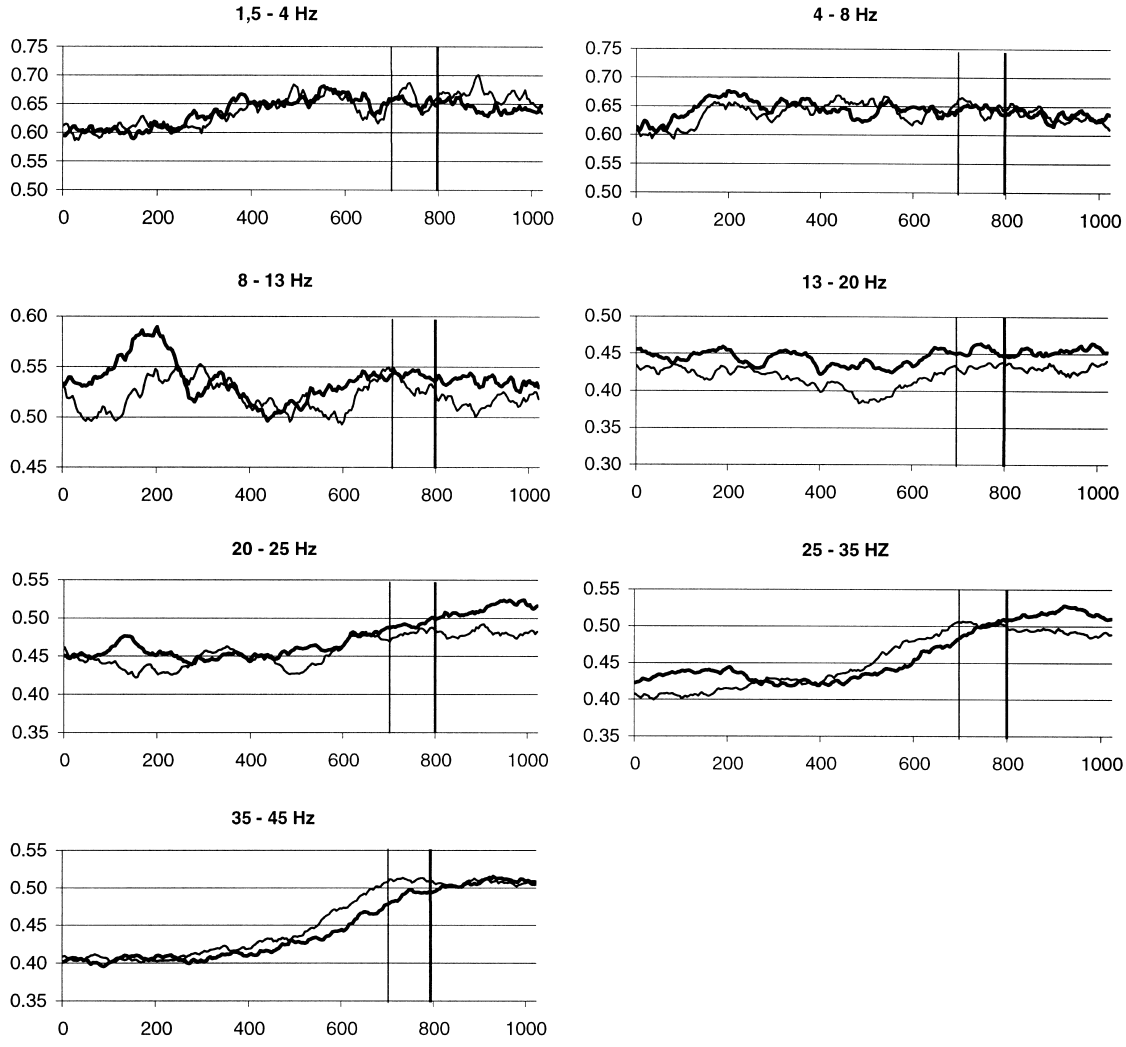

Fig. 3. Mean time courses of band coherences (in ms) of the incongruent (bold curves) and the congruent (thin curves) situations for the frequency bands 1.5–4, 4–8, 8–13, 13–20, 20–25, 25–35 and 35–45 Hz for the electrode pair F3/Pz. The thin vertical line denotes the mean reaction time for the congruent situation (708 ms), the thick vertical line denotes the mean reaction time for the incongruent situation (793 ms).

For a statistical validation, the mean values of the ERP for the time interval 450–550 ms were calculated for all electrode positions. The one-way ANOVA for all 19 electrode positions with the factor discriminating between the congruent and incongruent cases resulted in significant differences (significance level of 5%) for the electrode positions C3, C4, T5, P3, Pz, P4, T6, O1 and O2. No differences appear within the frontal area.

3.3. Coherence analysis

3.3.1. Choice of a sensitive frequency band for the discrimination between the two task situations

Given our hypotheses, differences in topography of coherence values between the congruent and the incongruent task will be searched primarily within the left frontal and within the left parietal area and also between the frontal and parietal areas.

In order to determine a sensitive frequency band in this regard mean time-coherence-analyses according to equation (Eq. (10)) in the Appendix were performed for the electrode pairs Fp1/F7, Fp1/F3, F7/F3, F3/Fz and F3/C3 within the left frontal area, for the electrode pairs Fp2/F8, Fp2/F4, F8/F4, F4/Fz and F4/C4 within the right frontal area, for the electrode pairs P3/C3, P3/Pz, P3/T5, P3/O1 and T5/O1 within the left parieto-temporal area, for the electrode pairs P4/C4, P4/Pz, P4/T6, P4/O2 and T6/O2 within the right parieto-temporal area and for the fronto-parietal electrode pairs F3/P3, F3/Pz, F4/P4 and F4/Pz.

The mean time-frequency-matrices of coherence were calculated for all 10 subjects and both task conditions. Afterwards, the difference (incongruent minus congruent situation) of the mean matrices was taken to find frequency bands with the highest differences. Fig. 2 shows these 3 mean matrices (incongruent case, congruent case and their difference) for the fronto-parietal electrode pair F3/Pz.

High coherences appear during the whole task for lower ($<$10 Hz) frequencies for both conditions. At the end of the

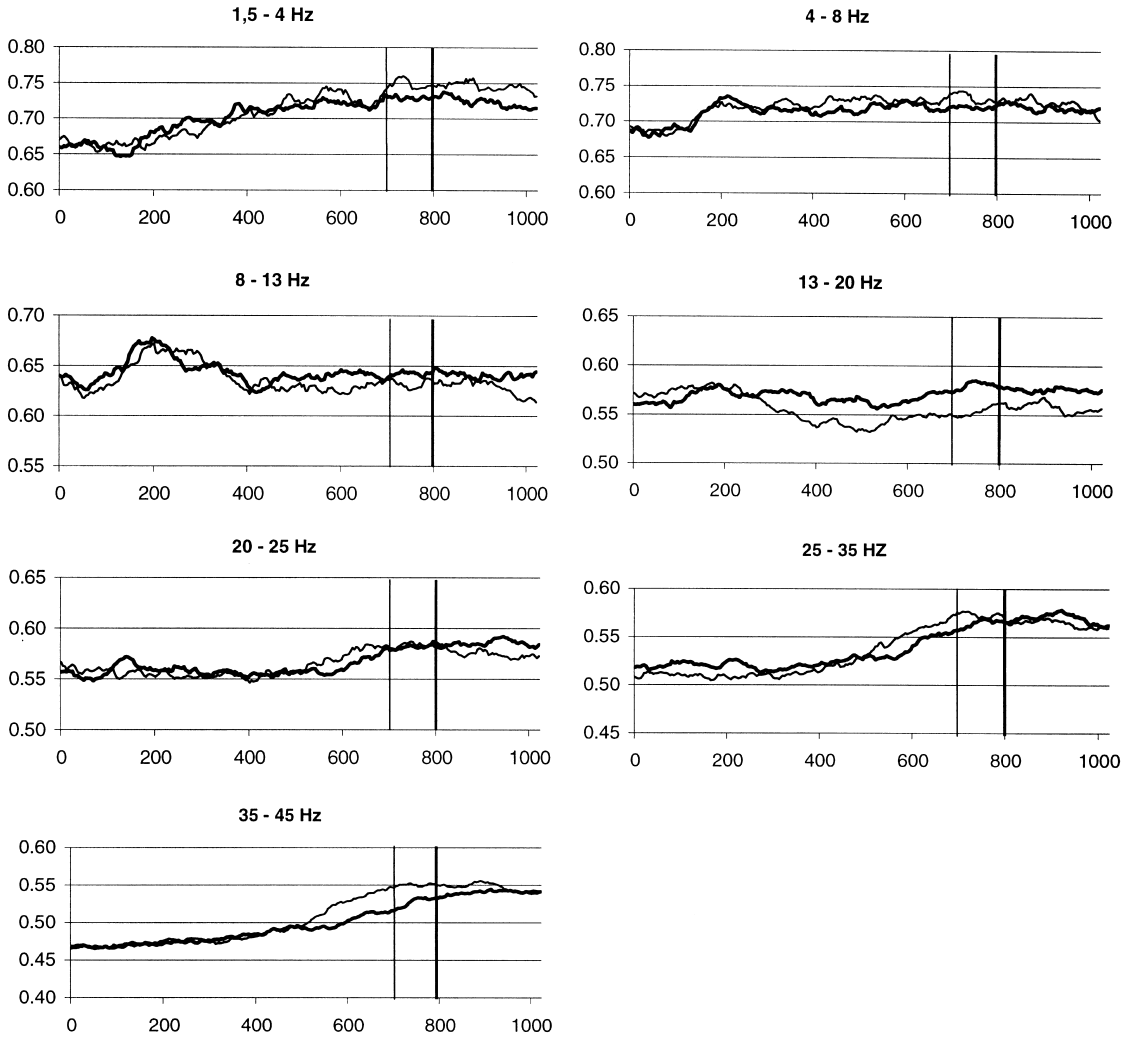

Fig. 4. Mean time courses of band coherences (in ms) of the incongruent (bold curves) and the congruent (thin curves) situations for the frequency bands 1.5–4, 4–8, 8–13, 13–20, 20–25, 25–35 and 35–45Hz averaged over the electrode pairs Fp1/F3, Fp1/F7, F7/F3, F3/Fz, F3/P3, F3/Pz, P3/Pz. The thin vertical line denotes the mean reaction time for the congruent situation (708 ms), the thick vertical line denotes the mean reaction time for the incongruent situation (793 ms).

task, an increase of the coherences may be seen especially around 30 and 40 Hz, again for both task conditions. For the time interval 400–700 ms, the highest differences between the two situations appear within the frequency band 13–20 Hz. On the right lower panel, the time course of the difference in band coherences (calculated according to Eq. 11 in the Appendix) for this frequency band is illustrated. There is a clear positive difference, approximately within the time interval from 300 ms by the end of the task.

For an objective rating of the sensitivity of different frequency bands, the mean time course (average for all 10 subjects) of band coherences for standard frequency bands and additional bands including the 30 Hz and 40Hz components were calculated according to Eqs. 10 and 11 in the Appendix for both congruent and incongruent situations. Fig. 3 shows these time courses of band coherences for the electrode pair F3/Pz.

The highest differences between both situations within the time interval, from 400 ms by the end of the task, appear within the frequency band 13-20 Hz. An increase of higher frequency band coherences (especially 25–35 Hz and 35–45 Hz) may be observed at the end of the task. Thereby, coherences increase earlier in the case of congruent situations than for incongruent situations. This phenomenon possibly could be explained by the smaller task duration and the earlier preparation on speech in the congruent case. The time-delay of these band coherences reaching a level between 0.45–0.5, seems to be the same as the time-delay in reaction times.

The observations described concern the coherences for one electrode pair, namely F3/Pz. Fig. 4 shows that they are valid for frontal and parietal areas of the left hemisphere.

In Fig. 4 the mean time courses of band coherences averaged over the electrode pairs Fp1/F3, Fp1/F7, F7/F3, F3/Fz, F3/P3, F3/Pz, P3/Pz of the left hemisphere are represented. Because of averaging the curves are smoother. But, the

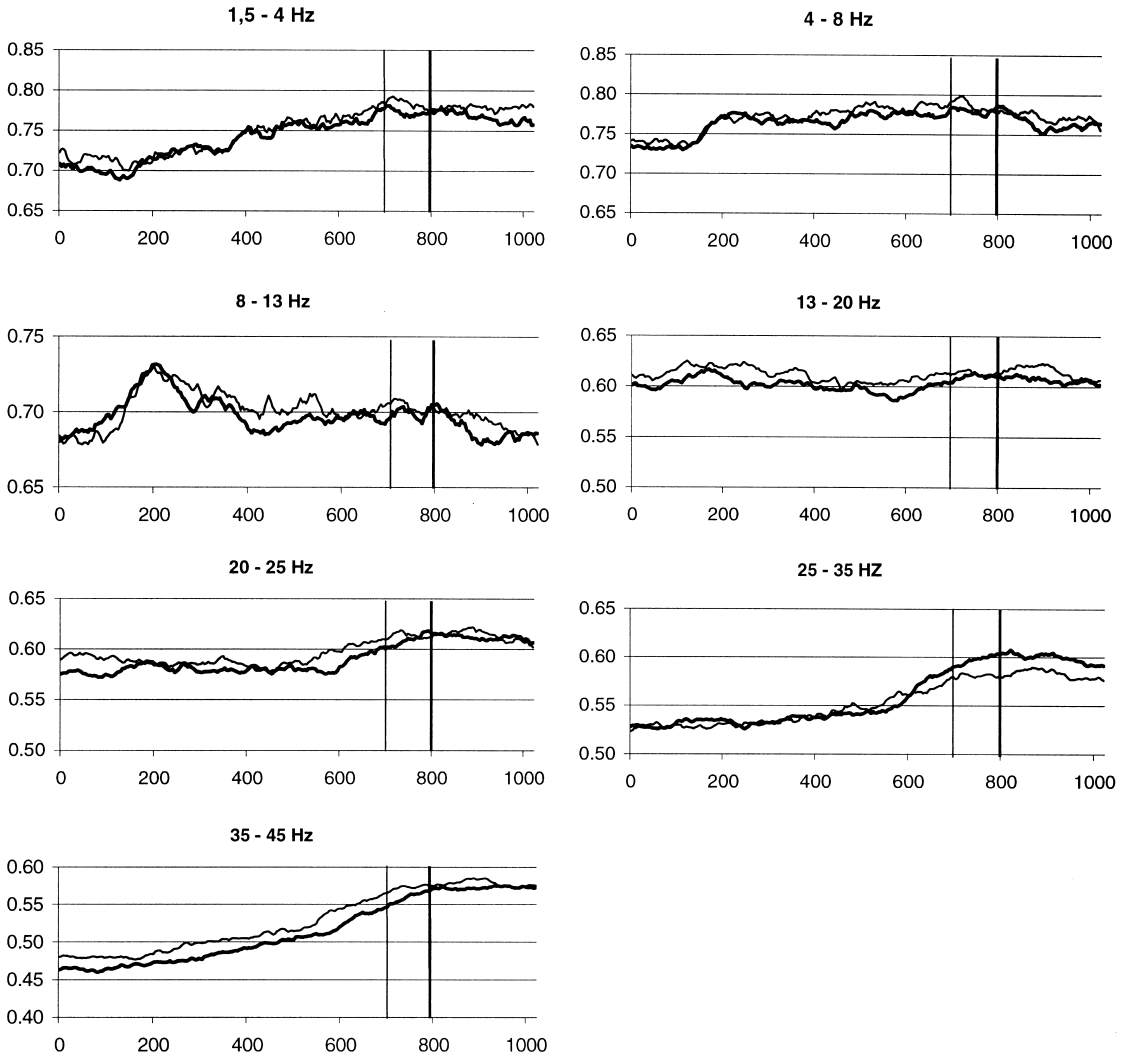

Fig. 5. Mean time courses of band coherences (in ms) of the incongruent (bold curves) and the congruent (thin curves) situations for the frequency bands 1.5–4, 4–8, 8–13, 13–20, 20–25, 25–35 and 35–45 Hz averaged over the electrode pairs Fp2/F4, Fp2/F8, F8/F4, F4/Fz, F4/P4, F4/Pz, P4/Pz. The thin vertical line denotes the mean reaction time for the congruent situation (708 ms), the thick vertical line denotes the mean reaction time for the incongruent situation (793 ms).

same effects may be observed here as they were for the single electrode pair F3/Pz. The highest difference of coherences between the incongruent and the congruent situation is visible within the frequency band 13–20 Hz.

We get a different picture for coherences of electrode pairs of the right hemisphere. In Fig. 5, the mean time courses of band coherences averaged over the electrode pairs Fp2/F4, Fp2/F8, F8/F4, F4/Fz, F4/P4, F4/Pz, P4/Pz of the right hemisphere are selected.

In contrast to the effect of the left hemisphere, the coherences are slightly higher in the congruent case for the frequency band 13–20 Hz (and also for the frequency band 35–45 Hz). The Stroop effect seems to be expressed as a lateralization effect of the synchronization phenomenon described by the coherence of the frequency band 13–20 Hz.

The investigation of averaged band coherences with regard to the discrimination between the two task situations indicate the frequency band of 13–20 Hz. For this reason, the frequency band of 13–20 Hz was chosen and fixed for further detailed statistical investigations.

3.3.2. Coherences within the time interval of late potentials

The local coherence mapping procedure was used to give a topographical overview of differences between local coherences in the incongruent and congruent situations. The continuous estimation procedure results from the sampling frequency of 250 Hz in a time resolution for instantaneous coherence of 4 ms. Therefore, it is possible to produce local coherence maps for every 4 ms. Fig. 6 shows the difference sequence of local instantaneous coherence maps with a time resolution of 20 ms (every 5 successive maps are averaged).

Starting with approximately 400 ms, strong positivity of

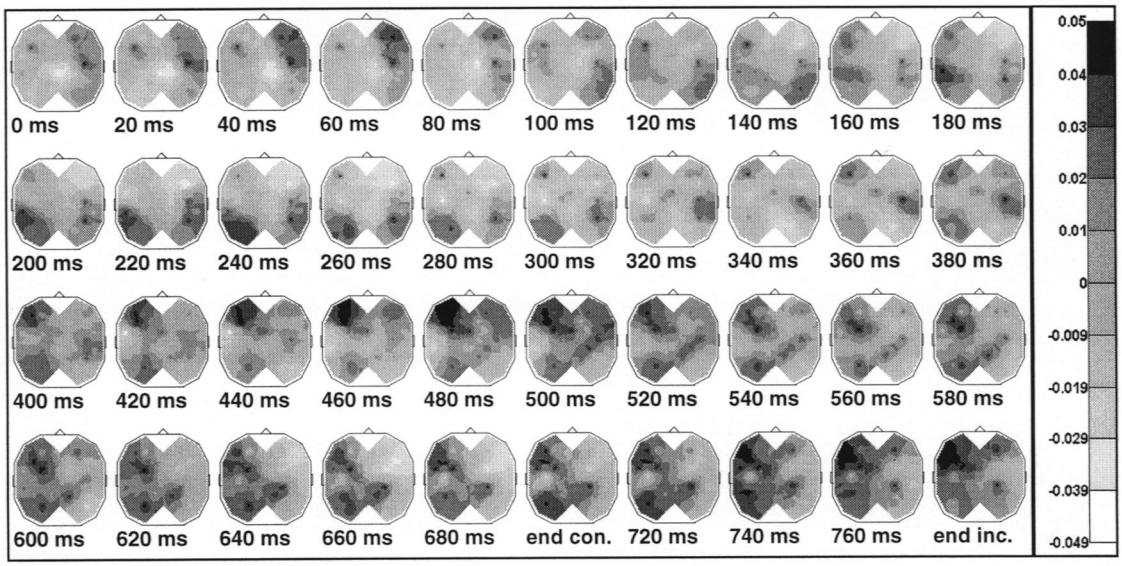

Fig. 6. Mean difference sequence (incongruent - congruent) of local coherence maps for ten subjects. The mean task-ends are denoted by end con. and end inc., respectively. The results showed higher local coherences for the incongruent task in the left frontal and left temporo-visual areas; in contrast, for the congruent task in the right parietal area.

difference may be observed within the left frontal area and slight positivity of difference within the left parietal area.

In order to concentrate on electrode pairs of the frontal and parietal regions which are of special interest in our hypotheses testing the electrode pairs Fp1/F7, Fp1/F3, F7/F3, F3/Fz, Fp2/F8, Fp2/F4, F8/F4, F4/Fz, F3/Pz, F4/Pz, P3/Pz and P4/Pz were selected to illustrate the mean time course of coherences. Thereby, the instantaneous band coherences (13–20 Hz) of the left frontal area Fp1/F7, Fp1/F3, F7/F3 and F3/Fz and of the right frontal area Fp2/F8, Fp2/F4, F8/F4 and F4/Fz were averaged over the correspondent regions. The global effect of higher local coherences (13–20 Hz) within the left frontal area for the incongruent situation in comparison with the congruent situation is depicted in Fig. 8, where the differences (incongruent minus congruent situation), sample point by sample point, are shown.

For the averaged coherences of the electrode pairs Fp1/F7, Fp1/F3, F7/F3 and F3/Fz within the left frontal area obvious higher positive differences appear within the left frontal area within the time interval 400 ms by the end of the task. This fact is completed by the higher fronto-parietal coherence F3/Pz within the same time interval for the incongruent case. For P3/Pz, positive differences also appear.

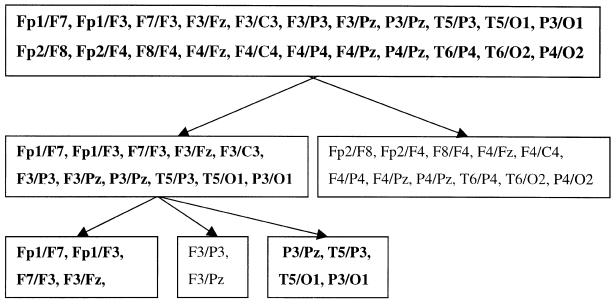

Fig. 7. Gradual application of the standardized sum test to mean band coherences (frequency band: 13–20 Hz; time interval: 400 ms by the end of the task). Sets of electrode pairs with significant difference between incongruent and congruent task situations with regard to mean band coherences are written in bold font.

There are no obvious differences between the two task conditions within the right frontal and parietal areas. In contrast to the positivity of the difference for the left fronto-parietal coherence F3/Pz we have a negative difference for the right fronto-parietal coherence F4/Pz.

For statistical verification, the mean coherences for the time interval from 400 ms after the stimulus by the end of the task were calculated for each subject (individual reaction times varied from 600–900 ms). Mean values of coherences for selected electrode pairs for both task conditions are listed in Table 1.

Afterwards, Fisher's z-transformation was applied to coherence values in order to enforce normality. Univariate *t* tests for paired samples provided significant differences of coherences between incongruent and congruent task situations mainly for electrode pairs of the left hemisphere (significance level of 5%). But, the execution of multiple statistical univariate tests may increase the possibility to obtain significance results by chance alone for alpha inflation. Therefore, the performance of multivariate tests is necessary.

Classical multivariate significance tests often are not feasible if the number of variables is greater than the number of observations. Thus, from the ANOVA no significant differences were obtained. Because of the high dimensionality Bonferroni or Holm correction was not suitable ditto. Therefore, a parametric test for multivariate data (Standardized Sum Test, SS test) was used (Läuter, 1996; Läuter et al., 1996).

Table 1
Mean band coherences (13–20 Hz) for the time interval 400 ms by the end of the task for frontal, parietal and fronto-parietal electrode pairs of the left and right hemisphere. Significant different coherence values are written in bold font (*t* test for paired samples of z-transformed coherence values with a significance level of 5%).

Left hemisphere				Right hemisphere			
Electrode pairs	Area	Incongr. task	Congr. task	Electrode pairs	Area	Incongr. task	Congr. Task
Fp1/F7	Left frontal	**0.43**	**0.37**	Fp2/F8	Right frontal	0.57	0.56
Fp1/F3		0.48	0.46	Fp2/F4		**0.50**	**0.47**
F7/F3		0.56	0.50	F8/F4		0.57	0.58
F3/Fz		0.79	0.77	F4/Fz		0.81	0.81
F3/C3		**0.61**	**0.56**	F4/C4		0.61	0.60
F3/P3	Left fronto-parietal	0.42	0.40	F4/P4	Right fronto-parietal	0.39	0.41
F3/Pz		**0.44**	**0.40**	F4/Pz		0.41	0.43
P3/Pz	Left parieto-temporal	0.83	0.82	P4/Pz	Right parieto-temporal	0.79	0.75
T5/P3		**0.70**	**0.67**	T6/P4		0.64	0.61
T5/O1		**0.64**	**0.61**	T6/O2		0.56	0.54
P3/O1		**0.71**	**0.68**	P4/O2		0.65	0.65

In the first step the SS test was performed for all 22 electrode pairs listed in the upper box of Fig. 7. This multivariate test resulted in a significant difference between incongruent and congruent situations ($\alpha = 5\%$). Afterwards, the SS test was executed for both particular hemispheres with 11 electrode pairs at each case. For the set of electrode pairs of the right hemisphere no significant difference could be obtained. The SS test for the set of electrode pairs of the left hemisphere provided significance of the difference between both task situations ($\alpha = 5\%$). The application of the SS test to subsets of electrode pairs (left frontal, parieto-temporal and fronto-parietal areas according to lower boxes in Fig. 7) led to *P*-values between 5 and 10% for the left frontal and for the left parieto-temporal area.

By means of the statistical analysis, the visual impression of Figs. 6 and 8 of higher coherences within the left frontal

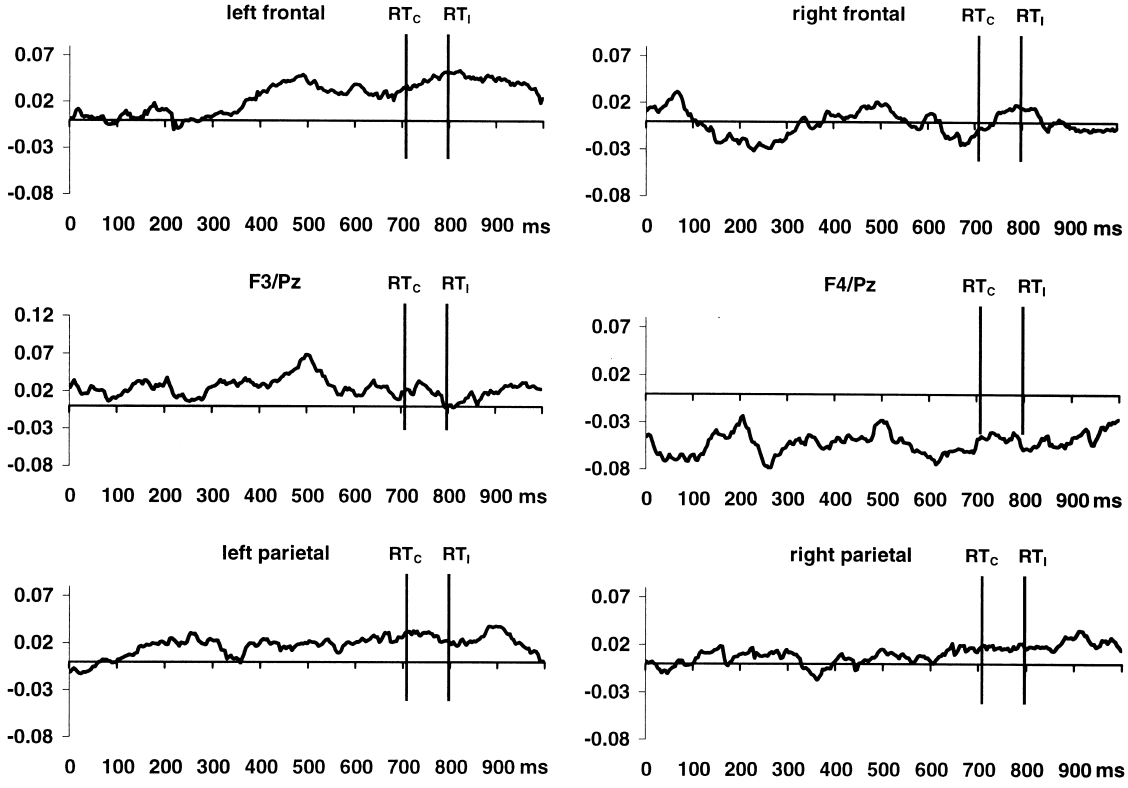

Fig. 8. Mean time courses of differences of band coherences (incongruent minus congruent task condition) for the frequency band 13–20 Hz. For the frontal areas the time courses were averaged over the electrode pairs Fp1/F7, Fp1/F3, F7/F3 and F3/Fz (upper left panel) and correspondingly over the electrode pairs Fp2/F8, Fp2/F4, F8/F4 and F4/Fz (upper right panel). The lower panels show the difference curves for the electrode pairs P3/Pz (left) and P4/Pz (right). The vertical lines denote the mean reaction time for the congruent situation ($RT_C = 708$ ms) and for the incongruent situation ($RT_I = 793$ ms).

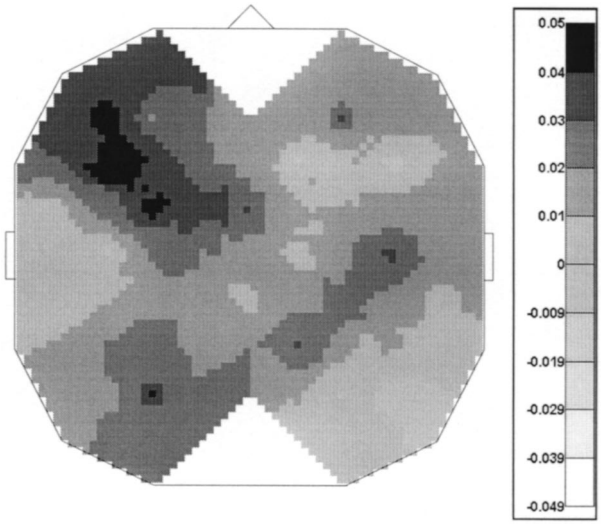

Fig. 9. Mean difference map (incongruent – congruent) of local coherences of the time interval 400 ms by the end of the task for 10 subjects.

and parietal areas for the incongruent case was confirmed in a global sense. For a topographical representation of this result the mapping procedure of local coherences was again carried out.

Fig. 9 illustrates the mean difference map of coherences for the time interval 400 ms by the end of the task (reaction time) and completes the results of Table 1. Obviously, in the case of the incongruent Stroop task there are higher local coherences for the electrode pairs in the left hemisphere and slightly lower local coherences for the electrode pairs in the right hemisphere within the second half of the task. We get equivalent results for the fronto-parietal electrode pairs. Differences in coherence of the electrode pairs F3/P3, F3/Pz, F3/P4 show positivity whereas differences in coherence of the electrode pairs F4/P3, F4/Pz, F4/P4 are negative. These results support our hypotheses of stronger interactions within and between the left frontal and parietal topographic areas.

3.4. Correlation between reaction time and time-point of maximal coherence

Using our time-continuous approach it is possible to look for connections between the chronometric behavioral parameters of the task and the characteristic time-events of the instantaneous band coherences. For this reason time-points of maximal coherences during the task were calculated for each of the 30 local and 9 fronto-parietal electrode pairs according to Eq. 12 in the Appendix. In order to avoid local maxima the time courses of band coherences were smoothed with a rectangular time window of 300 ms. Thereafter, the correlation coefficients between the mean time-points of maximal coherence and the mean reaction times of the 10 subjects were calculated for all 39 electrode pairs examined.

In the upper panels of Fig. 10, electrode pairs with significant correlation between time-points of maximal band coherence and reaction times are marked by arrows. In the case of the incongruent Stroop task there are high correlations within the left frontal, central and parietal regions as well as for 7 of the 9 fronto-parietal electrode pairs. In the congruent case there are high correlations above all in the right hemisphere. This impression of a lateralization effect will be mainly supported by the mapping of the correlation coefficients between the time-points of maximal coherence for 30 adjacent electrode pairs and the reaction times by themselves. These 'local correlation' maps are illustrated on the lower two panels of Fig. 10.

From Fig. 10 (panels one and two) it can be seen that a significantly high correlation exists between the time-points of maximal coherence and the reaction time for the four fronto-parietal electrode pairs F3/P3, F3/Pz, F4/Pz and F4/P4 in the incongruent case, whereas there is only a significantly high correlation between the time-points of maximal coherence and the reaction time for one of these 4 fronto-parietal electrode pairs in the congruent case, namely F4/P4. The concrete values of correlation coefficients are listed in Table 2.

The stronger correlation within the left hemisphere for the incongruent case in comparison with the congruent case and the equivalent strength of correlation within the right hemisphere for both situations are illustrated in the scatterplots in Fig. 12.

The average of fronto-parietal electrodes F3/P3 and F3/Pz represent the left hemisphere and the average of fronto-parietal electrodes F4/P4 and F4/Pz represent the right hemisphere, analogously.

3.5. The Stroop effect and the time evolution of interaction processes

Table 2 and Figs. 10 and 11 show the lateralization of strength of correlation between time-points of high synchronization described by coherence and the reaction time.

Furthermore, it is interesting for a procedural analysis to compare the absolute values of these time-points of maximal coherence for the two task conditions. The first main result is that the time-points of maximal coherences appear overall later for the incongruent Stroop task than for the congruent one. In Table 3, the time-points of maximal coherence are listed for selected electrode pairs of the frontal and parietal areas.

From Table 3 it may be observed that the peak of network synchronization, described by the coherence, appears later for the incongruent task. This is generally the case for all electrode pairs under consideration. Thereby, after performing the square root transform for time-points of maximal coherence to enforce normality, the one-way ANOVA results in significant time differences for the electrode pairs Fp1/F7, F3/P3, F3/Pz, F4/P4 and P4/Pz. Additionally, the univariate Wilcoxon test performed shows further significant differences. Thus, the time evolution of the inter-

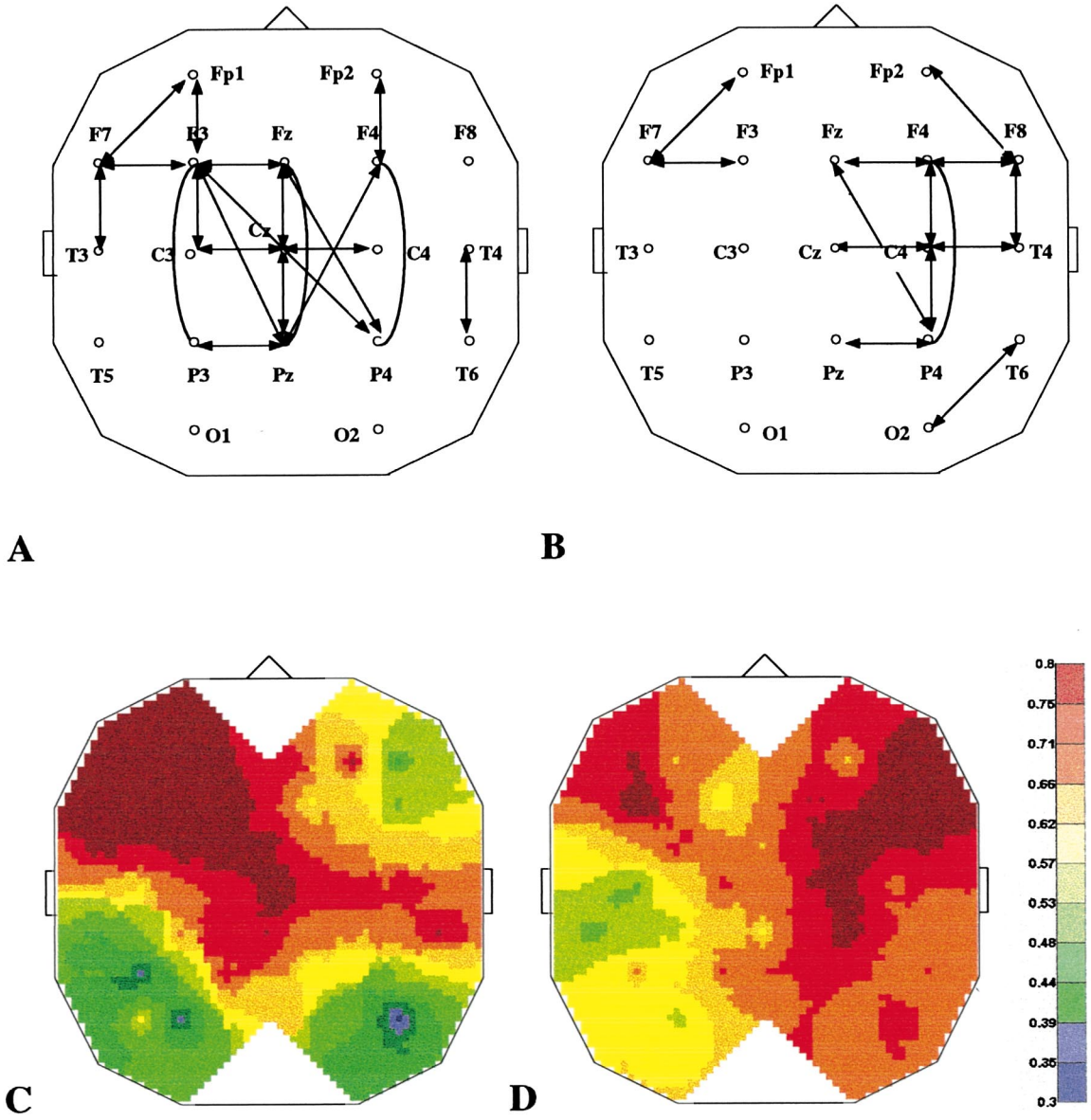

Fig. 10. Arrows and lines mark electrode pairs with significant high (1%) correlation (Pearson's correlation coefficient) between the time-points of maximal coherence and reaction time. (A) Incongruent Stroop task. (B) Congruent Stroop task. Maps of correlation coefficients: (C) Incongruent Stroop task. (D) Congruent Stroop task.

action processes described by instantaneous coherences of local and fronto-parietal electrode pairs are different for the congruent and incongruent task situations. A topographic overview of this general effect is given by the maps of time-points of maximal local coherences in Fig. 12.

Table 2
Pearson's correlation coefficient between time-point of maximal coherence and reaction time for the fronto-parietal electrode pairs F3/P3, F3/Pz, F4/Pz, F4/P4

Correlation between time-point of max. coherence and reaction time				
Situation	F3/P3	F3/Pz	F4/Pz	F4/P4
Incongruent	0.90[a]	0.97[a]	0.861[a]	0.781[a]
Congruent	0.55	0.62	0.68	0.81[a]

[a] Correlation is significant at the 0.01 level.

The scales (in ms) of the left and the middle maps of time-points of maximal coherence in Fig. 12 and also the scale of positive numbers only for their difference map (right), show that the time-points of maximal coherence come later for all adjacent electrode pairs in the incongruent case.

Further, from the left and the middle maps in Fig. 12 and from Table 3 it can be seen that the time of maximal synchronization appear later for the parietal electrode pairs P3/Pz and P4/Pz than for the electrode pairs within the frontal areas. Therefore, a MANOVA was performed with two steps for the task condition factor (congruent and

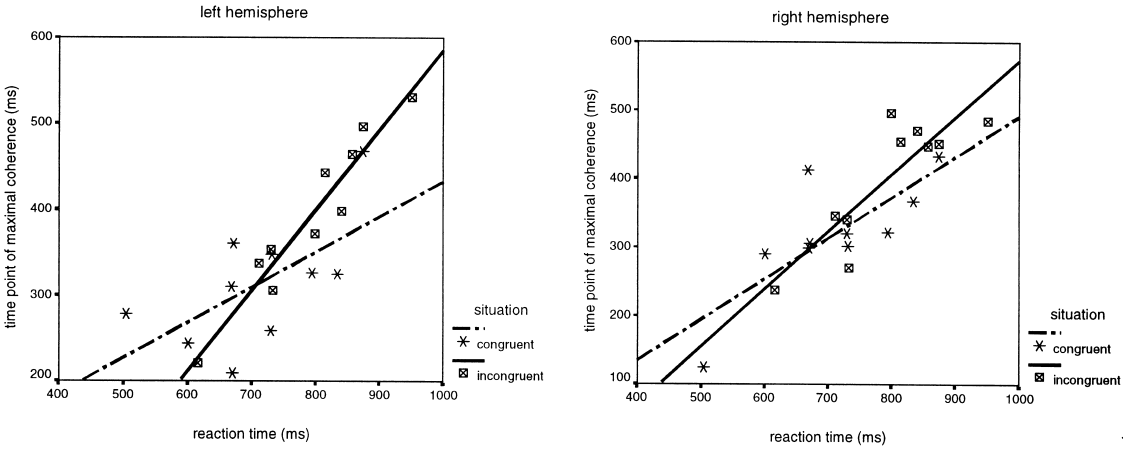

Fig. 11. Scatterplots between the time-points of maximal coherence of the average of the electrode pairs F3/P3 and F3/Pz and the reaction time (left panel) and correspondingly between the time-points of maximal coherence of the average of the electrode pairs F4/P4 and F4/Pz (right panel) for the incongruent and the congruent Stroop tasks, respectively.

incongruent) and two steps of the topographic area factor (parietal for P3/Pz and P4/Pz and frontal for F3/C3, F3/Fz, F7/F3, Fp1/F3, Fp1/F7, F4/C4, F4/Fz, F8/F4, Fp2/F4 and Fp2/F8) for all ten adjacent electrode pairs from Table 3. Again, a square root transformation was performed to enforce the normal distribution of the time-points of maximal coherence. For the task condition factor, the time-points of maximal coherence were higher (significance level of 5%) in the incongruent case for all 10 electrode pairs and for the topographic area factor the time-points of maximal coherence within the parietal area came later than those for the electrode pairs F3/C3, F7/F3, Fp1/F3, Fp1/F7 and Fp2/F4 (significance level at 5%). The results of a subsequent *t* test are listed in Table 4.

Evidently, the highest differences appear within the left hemisphere and for the congruent case. The peak of network synchronization within the left hemisphere described by the coherence of the correspondent electrode pairs appears later within the parietal area than within the frontal area. This fact speaks for the procedural behavior of the interaction process and indicates, possibly, a color-word perception.

Because of the sensitivity of these time-events it seems to be useful to calculate the values of maximal coherences by themselves. The calculation was done for every single trial. For each person these values were averaged individually for the two situations. Fig. 13 shows the mean difference map of maximal coherences for all 10 subjects.

For a statistical validation, analogously as in the case of mean band coherences, firstly univariate *t* tests for z-transformed maximal coherences were executed (see Table 5).

Afterwards, the multivariate SS test was performed to z-transformed values of maximal coherences for 22 electrode pairs listed in the upper box of Fig. 14.

The application of the global test for all electrode pairs resulted in a significant difference between incongruent and congruent task conditions ($\alpha = 10\%$). After subdividing the whole set of electrode pairs into two subsets according to Fig. 14, from the global test for 11 electrode pairs of the left hemisphere a significant difference was obtained ($\alpha = 5\%$),

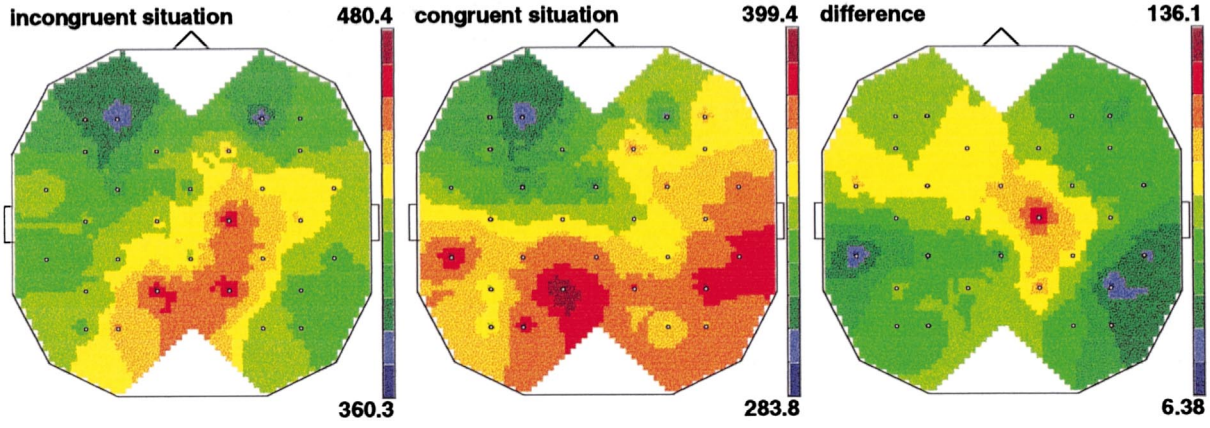

Fig. 12. Maps of time-points (in ms) of maximal coherence in the incongruent and congruent situations and of their differences (incongruent-congruent).

Table 3
Time-points of maximal coherence (ms) and their differences for selected electrode pairs. (Bold font denotes significant differences between incongruent and congruent situations on the basis of one-way ANOVA on the square root transformed values of time-points. Italicized font denotes additional significant differences on the basis of the Wilcoxon test for paired samples (significance level of 1%)

Time-points of maximal coherence (ms)							
Left hemisphere				Right hemisphere			
Electrode pairs	Incongr. Task	Congr. task	Difference	Electrode pairs	Incongr. task	Congr. task	Difference
Fp1/F7	*391*	*322*	*69*	Fp2/F8	*411*	*367*	*44*
Fp1/F3	**360**	**284**	**76**	Fp2/F4	*365*	*303*	*63*
F7/F3	*406*	*331*	*75*	F8/F4	*419*	*349*	*70*
F3/Fz	*424*	*335*	*89*	F4/Fz	*440*	*372*	*69*
F3/C3	394	310	84	F4/C4	430	370	60
F3/P3	**394**	**317**	**78**	F4/P4	**416**	**307**	**109**
F3/Pz	**389**	**308**	**82**	F4/Pz	383	327	56
P3/Pz	*473*	*399*	*74*	P4/Pz	**480**	**379**	**102**

whereas the global test for 11 electrode pairs of the right hemisphere showed no significant difference. The execution of the SS test for subareas (see Fig. 14) of the left hemisphere resulted in significant differences for the left parieto-temporal area only ($\alpha = 5\%$).

In comparison with the mean coherences at the end of the task there are, above all, higher differences within the left posterior hemisphere. This result indicates a stronger color-word perception in the incongruent task situation. Thus, the single trial-dependent detection of the time-point of maximal coherence increases the sensitivity of the discrimination between the congruent and the incongruent task within the left temporo-parietal area by means of instantaneous coherence.

4. Discussion

Coherence has been frequently used to investigate cognitive processes (Petsche et al., 1993; Petsche, 1996; Petsche and Etlinger 1998; Sarnthein et al., 1998).

Our previous studies have shown that an instantaneous approach increases the sensitivity of coherence when considering information processing (Schack and Krause, 1995; Krause et al., 1998; Schack et al., 1999a,b). The interference during incongruent Stroop tasks may be described in detail on the basis of this parameter. Values of coherence in the time interval of late potentials and values of maximal coherences in particular are quantitative parameters for distinguishing between the congruent and the incongruent cases. During incongruent Stroop tasks, high coherences within the frequency band 13–20 Hz appeared within the left frontal, central, and left parietal regions, and additionally for fronto-parietal electrode pairs in the left hemisphere. In contrast, in the congruent case, the coherence values in the right hemisphere increased in comparison to the incongruent case.

Additionally, the time-points of maximal coherence are qualitative parameters which demonstrate persuasively the close connection between the time evolution of the task and the behavior of the instantaneous coherence. The correlation between synchronization processes described by instantaneous coherence and the time evolution of the task quantified by the reaction time was very close in the incongruent case, whereas such correlations were restricted to the right hemisphere in the congruent case. The evolution of peak synchrony appeared earlier in the frontal areas than in the parietal area as listed in Table 3. This fact suggests the plausible early frontal 'executive functions' with subsequent synchrony in the parietal areas which indicates a

Table 4
Comparison of square-root transformed time-points of maximal coherence between the parietal electrode pairs P3/Pz and P4/Pz and selected frontal electrode pair positions corresponding to the left and right hemispheres

P-values of paired samples *t* test					
	P3/Pz			P4/Pz	
Electrode pairs	Incongruent task	Congruent task	Electrode pairs	Incongruent task	Congruent task
Fp1/F7	0.094	0.012	Fp2/F8	0.159	0.699
Fp1/F3	0.006	0.003	Fp2/F4	0.007	0.053
F7/F3	0.096	0.017	F8/F4	0.041	0.216
F3/Fz	0.088	0.023	F4/Fz	0.256	0.774
F3/C3	0.024	0.021	F4/C4	0.092	0.762

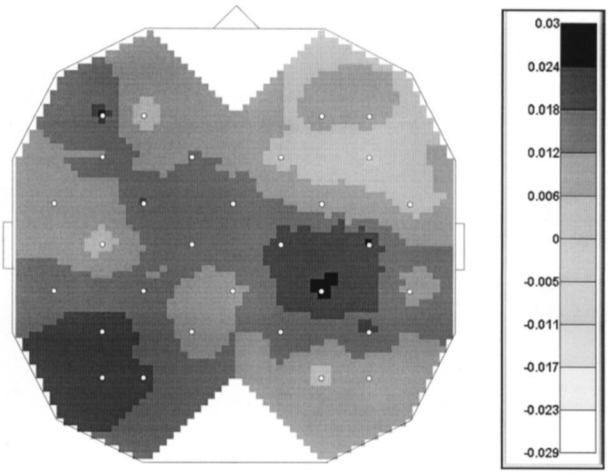

Fig. 13. Map of differences of values of maximal coherence (incongruent–congruent) for the frequency band 13–20 Hz.

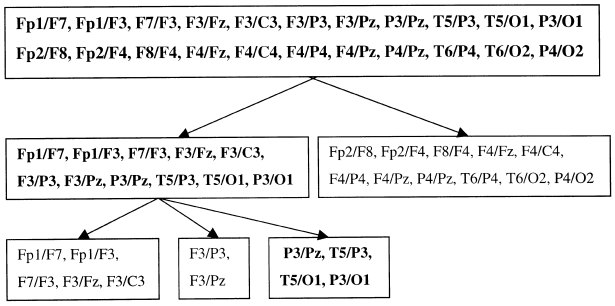

Fig. 14. Gradual application of the standardized sum test to maximal band coherences (13–20 Hz). Sets of electrode pairs with significant difference between incongruent and congruent task situations with regard to maximal coherences are written in bold font.

semantic memory retrieval in the parietal regions, similar to N400 components of linguistic ERP studies.

Furthermore, the topographic predications coincide with the results achieved on the basis of other investigation methods such as PET and MRI analysis (Bench et al., 1993; Taylor et al., 1994; Vrendell et al., 1995).

Similarities appeared with a previous ERP analyses of the Stroop task (Warren and Marsch, 1979; Czigler and Csibra, 1991; Hasenfratz and Bättig 1992; Soininen et al., 1995; Willis et al., 1996; West and Bell 1997) in relation to the late cognitive potentials as a sensitive time interval for the distinction between congruent and incongruent Stroop tasks. The discrimination between the incongruent and congruent task by means of ERP could only be shown for the posterial cortex in this study. The coherence analysis pointed out mainly the interaction phenomena of the Stroop effect within the left frontal area and between the left frontal and parietal areas. The investigation of chronometric correlation between the internal interaction process described by peak instantaneous coherence and the reaction time as external behavior data, support these results.

Modern neuroimaging methods like PET and fMRT opens possibilities of finding locations of sources for information processing. In contrast to these methods, coherence analysis enables the investigation of interaction processing for different topographic areas and thus adds a new aspect to the consideration of cognitive processes. The instantaneous approach used in this study additionally allows one to describe the procedural character of interaction processes for cognitive processes like the Stroop test, where fast changes with regard to interaction are expected.

All results described above were achieved with unipolar linked ears reference. The choice of a suitable derivation is one general problem in EEG analysis. Therefore, several authors have demonstrated that the reference also influences the value of coherence (Fein et al., 1988; Biggins et al., 1991; Lagerlund et al., 1995; Andrew and Pfurtscheller, 1996; Nunez et al., 1997; Essl and Rappelsberger, 1998 etc.). In order to avoid this influence, different 'reference-free' derivations as common average reference, bipolar derivations or different Laplacian derivation types has been used or constructed (Hjorth, 1975; Perrin et al., 1987, 1989;

Table 5
Maximal band coherences (13–20 Hz) for frontal, parietal and fronto-parietal electrode pairs of the left and right hemisphere. Significant different coherence values are written in bold font (t-test for paired samples of z-transformed coherence values with a significance level of 5%)

Left hemisphere				Right hemisphere			
Electrode pairs	Area	Incongr. task	Congr. task	Electrode pairs	Area	Incongr. Task	Congr. task
Fp1/F7	Left frontal	**0.56**	**0.53**	Fp2/F8	Right frontal	0.68	0.67
Fp1/F3		0.59	0.59	Fp2/F4		0.62	0.61
F7/F3		0.68	0.66	F8/F4		0.68	0.68
F3/Fz		0.86	0.84	F4/Fz		0.87	0.87
F3/C3		0.72	0.70	F4/C4		0.72	0.71
F3/P3	Left fronto-parietal	0.57	0.55	F4/P4	Right fronto-parietal	0.53	0.53
F3/Pz		**0.59**	**0.55**	F4/Pz		0.568	0.574
P3/Pz	Left parieto-temporal	0.88	0.86	P4/Pz	Right parieto-temporal	0.84	0.83
T5/P3		**0.79**	**0.77**	T6/P4		0.74	0.72
T5/O1		**0.75**	**0.72**	T6/O2		0.66	0.65
P3/O1		0.80	0.78	P4/O2		0.75	0.75

Perrin, 1992; Biggins et al., 1992; Pascual-Marqui, 1993; Law et al., 1993; Lagerlund et al., 1995 etc.).

Nunez et al. (1997) examined and compared coherence estimates with regard to different derivations. He recommended solving the problem of choosing the reference in order to provide the most robust indicators of clinical or cognitive state for each study individually. Nunez (1997) argued that average reference, cortical image and reduced coherencies behave in way that are qualitatively similar to reference coherence when large regions are compared.

In this context a strong topographic interpretation of our results seems to be not advisable. Independent of this fact, the major aim of the study, namely a clear discrimination between the congruent and incongruent task situations on the basis of instantaneous coherence parameters as described above, could be fulfilled.

Because the Stroop effect is very robust under changes in experimental conditions and contains elements of selective attention, word-reading, and color-naming processes, it is useful for testing a variety of cognitive theories. Thus, the Stroop effect continues to be important in psychology and is the goal of many cognitive models (Cohen et al., 1992; Mewhort et al., 1992; Sugg and McDonald, 1994).

Further, the results found in this study with regard to interaction phenomena connected with the Stroop effect may be helpful for the more certain indication of dysfunctions in patients without clear focal lesions.

5. Appendix

The adaptive estimation procedure of instantaneous coherence was conducted in two steps as follows: the first step was the adaptive fitting of a linear model to a pair of EEG channels. Let

$$\mathrm{x} = \left\{\left(\mathrm{x}_i^1 \mathrm{x}_i^2\right)^T\right\}_{i=0,1,2,\ldots}$$

be the sample values of two channels of an EEG record, where

$$\left(\mathrm{x}_i^1 \mathrm{x}_i^2\right)^T = \begin{pmatrix} \mathrm{x}_i^1 \\ \mathrm{x}_i^2 \end{pmatrix}^T$$

and i denotes the number of the sample value. This two-dimensional EEG signal was fitted by a two-dimensional autoregressive moving average (ARMA) model with time-varying parameters:

$$\mathrm{y}_n + \sum_{k=1}^{p} \mathrm{A}^k(\mathrm{n})\mathrm{y}_{n-k} = \mathrm{z}_n - \sum_{j=1}^{q} \mathrm{B}^j(\mathrm{n})\mathrm{z}_{n-j} \tag{1}$$

where p and q are the orders of the model, **z** is a two-dimensional independent white noise process, **y** is the two-dimensional model process, and $\mathbf{A}^k(n)$ and $\mathbf{B}^l(n)$ are 2*2- matrices of the autoregressive and moving average parameters. The minimization of the momentary quadratic prediction error of the model leads to the following adaptive estimation procedure for the parameter matrices:

$$\hat{\mathrm{A}}^k(\mathrm{n}) = \hat{\mathrm{A}}^k(n-1) - \mathrm{c}_n \mathrm{e}_n \mathrm{x}_{n-k}^T; \mathrm{k} = 1, \ldots, p$$

$$\hat{\mathrm{B}}^j(\mathrm{n}) = \hat{\mathrm{B}}^j(n-1) - \mathrm{c}_n \mathrm{e}_n \mathrm{e}_{n-j}^T; j = 1, \ldots, q \tag{2}$$

where $\{\mathrm{e}_n\}_{n=1,2,\ldots}$ is the estimated vector sequence of the prediction error:

$$\mathrm{e}_0 = 0$$

$$\mathrm{e}_n = \mathrm{x}_n - \mathrm{y}_n$$

$$= \mathrm{x}_n + \sum_{k=1}^{p} \hat{\mathrm{A}}^k(n-1)\cdot\mathrm{x}_{n-k} + \sum_{j=1}^{q} \hat{\mathrm{B}}(n-j)\cdot\mathrm{e}_{n-j}^T \tag{3}$$

The algorithm in Eqs. (2,3) is a generalization of the LMS algorithm for adaptive filtering of one-dimensional signals by autoregressive models for the case of adaptive filtering of multi-dimensional signals by autoregressive moving-average models. The time-varying stepwidth c_n was chosen reciprocally proportional to the sum of momentary variances of the two EEG signals (for details see Schack et al., 1999a). This signal-dependent determination of the stepwidth c_n guarantees the stability of the adaptive estimation procedure. The model order (p,q) was established in accordance with the Hannan criterion (Hannan and Kavalieris, 1984).

The second step of the adaptive estimation procedure consists of the parametric calculation of the spectral density matrix for each sample point. The momentary transfer function $\mathrm{H}_n(\lambda)$ of the fitted ARMA model may be calculated by the formula

$$\mathrm{H}_n(\lambda) = \mathrm{A}_n^{-1}(\lambda) * \mathrm{B}_n(\lambda), \tag{4}$$

with the momentary parameter matrices

$$\mathrm{A}_n(\lambda) = \mathrm{I} + \sum_{k=1}^{p} \hat{\mathrm{A}}^k(n) e^{-ik\lambda} \qquad \textit{and}$$

$$\mathrm{B}_n(\lambda) = \mathrm{I} - \sum_{k=1}^{q} \hat{\mathrm{B}}^j(\mathrm{n}) \mathrm{e}^{-ij\lambda}. \tag{5}$$

The momentary covariance matrix $\mathbf{S}_n$ of the bivariate prediction error $\{\mathrm{e}_n\}_{n=1,2,\ldots}$ may also be estimated in an adaptive manner according to:

$$\mathrm{s}_{ij}(0) = 0$$

$$\mathrm{s}_{ij}(n) = \mathrm{s}_{ij}(n-1) - \mathrm{c}_\mathrm{s}\cdot\left(\mathrm{s}_{ij}(n-1) - \mathrm{e}_n^i \cdot \mathrm{e}_n^j\right),\ i = 1, 2;\ n = 1, 2, \ldots \tag{6}$$

where c_s is a constant with $0 < \mathrm{c}_\mathrm{s} < 1$. It is now possible to calculate the spectral density matrix at every sample point n by

$$\mathrm{f}_n(\lambda) = \mathrm{H}_n(\lambda) * \mathrm{S}_n * \mathrm{H}_n^{*T}(\lambda), \tag{7}$$

where H_n^{*T} denotes the complex conjugate and transpose of $H_n(\lambda)$. This means that this adaptively estimated spectral density matrix

$$f_n(\lambda) = \begin{pmatrix} f_{11,n}(\lambda) & f_{12,n}(\lambda) \\ f_{21,n}(\lambda) & f_{22,n}(\lambda) \end{pmatrix}$$

is a function in frequency and in time. In such a way, we obtain the instantaneous quadratic coherence function at every sample point:

$$\hat{\rho}_n^2(\lambda) = \frac{|f_{12,n}(\lambda)|^2}{f_{11,n}(\lambda) * f_{22,n}(\lambda)}. \quad (8)$$

Because of the high variability of the EEG, and therefore of the adaptive EEG coherence, it is often necessary to estimate a mean time coherence analysis. For this purpose the following estimation procedure was executed. The ARMA model parameter matrices with time-dependent parameters are fitted for each single trial m, $m = 1, \ldots, M$, according to the adaptive estimation procedure (1)–(3):

$$\hat{A}_m^k(n) = \hat{A}_m^k(n-1) - c_n e_{m,n} x_{m,n-k}^T; k = 1, \ldots, p$$

$$\hat{B}_m^j(n) = \hat{B}_m^j(n-1) - c_n e_{m,n} e_{m,n-j}^T; j = 1, \ldots, q \quad (9)$$

Afterwards, the time-frequency-matrices for momentary coherence have to be calculated for each single trial according to Eqs.(4)–(8) and then averaged:

$$\bar{\rho}_n^2(\lambda) = \frac{1}{M} \sum_{m=1}^{M} \hat{\rho}_n^2(\lambda) \quad (10)$$

In this way we get a mean time-coherence-analysis for a cognitive operation which is assumed to be repeatable.

The limitation to sensitive frequency bands enables a necessary data reduction. As a result we get the time curve of mean band coherence. For a chosen frequency band $[\lambda_{low}, \lambda_{upper}]$ the mean band coherence is computed by

$$\hat{\rho}_{i,j}^2(n) = \frac{1}{\text{card}} \sum_{\lambda_{low} \le \lambda_k \le \lambda_{upper}} \hat{\rho}_{n;i,j}^2(\lambda_k) \quad (11)$$

for each sample point n and arbitrary EEG channel pair (i, j). The number of discrete frequency points with $\lambda_{low} \le \lambda_k \le \lambda_{upper}$ is denoted by card. The instantaneous mean band coherence (Eq. 11) can be regarded as a stochastic process by itself which is bounded by 0 and 1. Now it is possible to detect phases of high synchronization by smoothing the time curve (Eq. 11) and finding the time-point of maximal coherence t_C for any time interval $[t_1,t_2]$ of interest:

$$\hat{\rho}_{i,j}^2(t_c) \ge \hat{\rho}_{i,j}^2(t), \forall t \in [t_1, t_2]. \quad (12)$$

Furthermore, the value

$$\hat{\rho}_{i,j}^2(t_c)$$

indicates the intensity of maximal synchronization.

Acknowledgements

The authors would like to thank W. Krause for helpful suggestions and discussions and G. Grieszbach, J. Bolten and E. Möller for help in programming. (This study was supported by the Federal Ministry of Research and Technology (BMBF 01ZZ9602, DFG Scha 741/1-1 and DFG Scha 741/1-2).

References

Andrew C, Pfurtscheller G. Dependence of coherence measurements on EEG derivation type. Med Biol Eng Comput 1996;34:232–238.

Bench CJ, Frith CD, Grasby PM, Friston KJ, Paulesu E, Frackowiak RSJ, Dolan RJ. Investigations of the functional anatomy of attention using the stroop test. Neuropsychologia 1993;31:907–922.

Biggins CA, Fein G, Raz J, Amir A. Artifactually high coherences result from using spherical spline computation of scalp current density. Electroenceph clin Neurophysiol 1991;79:413–419.

Biggins CA, Ezekiel F, Fein G. Spline computation of scalp current density and coherence: a reply to Perrin. Electroenceph clin Neurophysiol 1992;83:172–174.

Cohen JD, Servan-Schreiber D, McCelland JL. A parallel distributed processing approach to automaticity. Am J Psychology 1992;105:239–268.

Czigler I, Csibra G. Event-related potentials in a lexical stroop task. Int J Psychophysiol 1991;11:281–293.

Essl M, Rappelsberger P. EEG coherence and reference signals: experimental results and mathematical explanations. Med Biol Eng Comput 1998;36:1–8.

Fein G, Raz J, Brown FF, Merrin EL. Common reference coherence data are confounded by power and phase. Electroenceph clin Neurophysiol 1988;69:581–584.

Hannan EJ, Kavalieris L. Multivariate linear time series models. Biometrika 1984;69:81–94.

Hasenfratz M, Bättig K. Action profiles of smoking and caffeine: stroop effect. EEG, and periphal physiology. Pharmacol Biochem Behav 1992;42:155–161.

Hjorth B. An on-line transformation of EEG scalp potentials into orthogonal source derivations. Electroenceph clin Neurophysiol 1975;39:526–530.

Hock HS, Egeth H. Verbal interference with encoding in a perceptual classification task. J Exp Psychol 1970;83:299–303.

Keele SW. Attention demands of memory retrieval. J Exp Psychol 1972;93:245–248.

Krause W, Gibbons H, Schack B. Concept activation and coordination of activation procedure require two different networks. NeuroReport 1998;9:1649–1653.

Lagerlund TD, Sharbrough FW, Busacker NE, Cicora KM. Interelectrode coherences from nearest-neighbor and spherical harmonic expansion computation of laplacian of scalp potential. Electroenceph clin Neurophysiol 1995;95:178–188.

Läuter J, Glimm E, Kropf S. New multivariate tests for data with an inherent structure. Biom J 1996;38:5–23.

Läuter J. Exact t- and F-tests for analysing studies with multiple endpoints. Biometrics 1996;52:964–970.

Law SK, Nunez PL, Wijesinghe RS. High-resolution EEG using spline generated surface laplacians on spherical and ellipsoidal surfaces. IEEE Trans Biomed Eng 1993;40(2):145–153.

Mewhort DJK, Braun JG, Heathcote A. Response time distributions and the stroop task: a test of the Cohen, Dunbar, and McClelland (1990) model. J Exp Psychol 1992;18:872–882.

Morton J. Categories of interference: verbal mediation and conflict in card sorting. Br J Psychol 1969;60:329–346.

Nunez PL, Srinivasan R, Wijesinghe RS, Westdorp AF, Tucker DM, Silberstein RB, Cadusch PJ. EEG Coherency I: statistics, reference electrode, volume conduction, laplacians, cortical imaging, and interpretation at multiple scales. Electroenceph clin Neurophysiol 1997;103:499–515.

Nunez PL, EEG coherence measures in medical and cognitive science: a general overview of experimental methods, computer algorithms, and accuracy. In: Witte H, Zwiener U, Schack B, Doering A, editors. Quantitative and topological EEG and MEG analysis. Druckhaus Mayer Verlag GmbH Jena Erlangen, 1997:385–392. ISBN 3-925978-67-4.

Pascual-Marqui RD, et al. The spherical spline Laplacian does not produce artifactually high coherences: comments on two articles by Biggins. Electroenceph clin Neurophysiol 1993;87:62–64.

Perrin F, Bertrand O, Pernier J. Scalp current density mapping: value and estimation from potential data. IEEE Trans Biomed Eng 1987;34(4): 283–288.

Perrin F, Pernier J, Bertrand O, Echallier JF. Spherical splines for scalp potential and current density mapping. Electroenceph clin Neurophysiol 1989;72:184–187.

Perrin F, et al. Comments on article by Biggins. Electroenceph clin Neurophysiol 1992;83:171–172.

Petsche, H., Etlinger, S.C., EEG and thinking. Verlag der Österreichischen Akademie der Wissenschaften. Wien, 1998.

Petsche H, Etlinger SC, Filz O. Brain electric mechanisms of bilingual speech administration: an initial investigation. Electroenceph clin Neurophysiol 1993;96:281–304.

Petsche H. Approaches to verbal, visual and musical creativity by EEG coherence analysis. Int J Psychophysiol 1996;24:145–160.

Posner MJ, Snyder CRR. Attention and cognitive control. In: Solso RL, editor. Information processing and cognition: the Loyola symposium, Hillsdale, NJ: Erlbaum, 1975.

Rappelsberger P, Petsche H. Probability mapping. Power and coherence analysis of cognitive processes. Brain Topogr 1988;1:46–54.

Sarnthein J, Petsche H, Rappelsberger P, Shaw GL, von Stein A. Synchronization between prefrontal and posterior association cortex during human working memory. Proc Natl Acad Sci USA 1998;95:7092–7096.

Schack B, Krause W. Dynamic power and coherence analysis of ultra short-term cognitive processes – a methodical study. Brain Topogr 1995;8:127–136.

Schack B. Dynamic topographic spectral analysis of cognitive processes. In: Uhl Ch, editor. Analysis of neurophysiological brain functioning, Berlin: Springer, 1999. pp. 230.

Schack B, Grieszbach G, Arnold M, Bolten J. Dynamic cross-spectral analysis of biological signals by means of bivariate arma processes with time-dependent coefficients. Med Biol Eng Comput 1995;33: 605–610.

Schack B, Grieszbach G, Krause W. The sensitivity of instantaneous coherence for considering elmentary comparison processing. Part I: the relationship between mental activities and instantaneous EEG coherence. Int J Psychophysiol 1999;31:219–240.

Schack B, Grieszbach G, Nowak H, Krause W. The sensitivity of instantaneous coherence for considering elementary comparison processing. Part II: similarities and differences between EEG and MEG coherences. Int J Psychophysiol 1999;31:241–259.

Seymour PHK. Stroop interference with response, comparison, and encoding stages in a sentence-picture comparison task. Memory Cognition 1974;2:19–26.

Seymour PHK. Conceptual encoding and locus of the Stroop effect. Q J Exp Psychol 1977;29:245–265.

Soininen HS, Karhu J, Partanen J, Pääkönen A, Jousmäki V, Hänninen T, Hallikainen M, Partanen K, Laakso MP, Koivisto K, Riekkinen PJ. Habituation of auditory N100 correlates with amygdaloid volumes and frontal functions in age-associated memory impairment. Physiol Behav 1995;57:927–935.

Stroop JR. Studies of interference in serial verbak reactions. J Exp Psychol 1935;18:643–661.

Sugg MJ, McDonald JE. Time course of inhibition in color-response and word-response versions of the stroop task. J Exp Psychol 1994;20:647–675.

Taylor SF, Kornblum S, Minoshima S, Oliver LM, Koeppers RA. Changes in medial cortical blood flow with a stimulus-response comparability task. Neuropsychologia 1994;32:249–255.

Vrendell P, Junque C, Pujol J, Jurado MA, Molet J, Grafman J. The role of prefrontal regions in the stroop task. Neuropsychologia 1995;3:341–352.

Warren LR, Marsch GR. Changes in event-related potentials during processing of stroop stimuli. Intern J Neurosci 1979;9:217–223.

Warren RE. Stimulus encoding and memory. J Exp Psychol 1972;94:90–100.

West R, Bell MA. Stroop color-word interference and electroencephalogram activation: evidence for age-related decline of the anterior attention system. Neuropsychology 1997;11:421–427.

Willis J, Nelson A, Black W, Borges A, An A, Rice J. Barbiturate anticonvulsants: a neuropsychological and quantitative electroencephalographic study. J Child Neurol 1996;12:169–171.